Chemical Engineering Journal Advances 18 (2024) 100603

Contents lists available at ScienceDirect

Chemical Engineering Journal Advances

journal homepage: www.sciencedirect.com/journal/chemical-engineering-journal-advances

Hydrodynamic cavitation effects on advanced oxidation processes and mass transfer: A conceptual model

S.N. Fleite [a,b,c], M.A. Ayude [d,e], V.V. Ranade [f], M.C. Cassanello [a,b,*]

[a] Instituto de Tecnología de Alimentos y Procesos Químicos (ITAPROQ) – CONICET/Universidad de Buenos Aires, Argentina
[b] Laboratorio de Reactores y sistemas para la Industria (LARSI), Departamento de Industrias, FCEyN, Universidad de Buenos Aires, Argentina
[c] Cátedra de Química Inorgánica y Analítica, Facultad de Agronomía, Universidad de Buenos Aires, Argentina
[d] División Catalizadores y Superficies , Instituto de Investigaciones en Ciencia y Tecnología de Materiales (INTEMA) – CONICET/UNMdP, Argentina
[e] Departamento de Ingeniería Química y de Alimentos, Universidad Nacional de Mar del Plata (UNMdP), Argentina
[f] University of Limerick, Ireland

ARTICLE INFO

Keywords:
Hydrodynamic cavitation
Supercritical water
Advanced oxidation processes
Conceptual model

ABSTRACT

Advanced oxidation process (AOPs) technologies are the subject of intense research due to the need for treating refractory wastewaters. Among them, hydrodynamic cavitation (HC) is particularly well-studied because of its potential as an AOP and as a means of intensification for other processes, including other AOPs. Understanding HC and its effects is crucial for its development and practical application. This study introduces a conceptual model that integrates the presence of supercritical water (SCW) to interpret HC results. The model was validated by selected experimental scenarios focused on exploring the impact of HC on the viscosity of a soluble polymer solution, the precipitation of an ionic salt from an unsaturated solution, and the stripping of volatile organic compounds (VOCs). The results were analyzed and interpreted using the conceptual model, remarking the scenarios that cannot be explained by the generally accepted mechanisms of radicals' formation or pyrolysis. Furthermore, the model was then applied to analyze the trends reported in the existing literature regarding the application of HC as an AOP and as a method of intensification. The occurrence of SCW as a key driving force for HC chemical and physical effects represents a novel approach with the potential to enhance the design and operation of HC systems, particularly when tailoring operating conditions to maximize SCW occurrence.

1. Introduction

Hydrodynamic cavitation (HC) has been a major research subject for the last decades. Initially investigated to understand the destructive effects of cavitation [47], it is now primarily studied due to HC potential benefits, especially when applied as an advanced oxidation process or as a means of intensification for other processes [16,40]. The main theories explaining HC effects are based on the extreme conditions reached when cavitation bubbles implode, leading to local temperatures exceeding 5000 K and pressures over 1000 bar due to the sudden bubble shrinkage and collapse [22,49]. These conditions create an excellent environment to promote the formation of radicals, especially hydroxyl radicals (HO•), known for their high reactivity in non-selectively oxidizing different compounds [9,42].

In addition to radical formation, another generally accepted mechanism, arising from the high temperatures achieved, is the pyrolysis of organic compounds inside the cavitation bubbles [5]. However, the radical-based approach has been dominant in the literature for explaining hydrodynamic cavitation effects as well as hybrid technologies that combine cavitation with other advanced oxidation processes [10,30]. Trends observed in the performance of HC at different values of pH have been explained by considering factors related to the rates of HO• formation and scavenging, as well as the dissociation equilibrium of organic compounds, affecting their distribution between gas and liquid phases inside and outside the cavitation bubbles [7]. Furthermore, it was proposed that an optimum HC condition can be estimated by considering the maximum collapse velocity related to the rates of HO• generation [31,34,54]. Synergistic effects observed in hybrid processes have been attributed to the intensified formation of radicals and enhanced mass transfer in the liquid phase resulting from the extreme turbulence induced by cavitation [10].

Though usually overlooked, the influence of thermodynamics during

---

* Corresponding author.
E-mail address: miryan@di.fcen.uba.ar (M.C. Cassanello).

https://doi.org/10.1016/j.ceja.2024.100603

the collapse, specifically the aggregate state of matter inside the cavitation bubble (liquid, gas, and/or the phase under supercritical conditions) needs to be considered in HC experiments. Extreme temperatures and pressures achieved due to bubble implosion can locally lead to the formation of supercritical phases. The presence of a supercritical phase can strongly modify the interphase mass transfer and impact the HO• generation and/or pyrolysis mechanisms. Thus, the existence of supercritical domains would be a plausible alternative mechanism and/or have a non-negligible effect on the generally accepted ones.

In the case of aqueous solutions, supercritical water (SCW) can be formed. SCW exhibits distinct physical properties compared to liquid water under ambient or subcritical conditions, including weakened hydrogen bonds, a lower dielectric constant, and higher diffusion coefficients [55]. It resembles more an organic solvent than liquid water; thus, SCW results in lower solubility for ionic compounds like salts, and increased solubility of gases and nonpolar organic compounds. This makes SCW a medium that accelerates certain chemical reactions compared to liquid water. For instance, it promotes HO• formation and reactivity [11] and enhances oxidation processes driven by gas oxidants such as oxygen or ozone due to reduced mass transfer limitations [55]. These trends highlight the similarities between the effects of SCW and HC and the importance of determining the potential influence of SCW domains on HC through simulations and experiments.

This work aims to explore the occurrence of SCW in HC and propose a conceptual model incorporating SCW presence to elucidate the effects of bubble collapse dynamics. First, the operating conditions and outputs in cavitation systems are compared with those in SCW oxidation reactors. Then, experiments of HC are conducted at the optimum inlet pressure on aqueous solutions of carboxymethylcellulose, $BaSO_4$, or ethanol and hexanol. These compounds were selected as models of polymeric, ionic, and volatile organic compounds (VOCs), respectively, to illustrate the generalizability of the hypothesis to different scenarios.

2. Methods

2.1. Experimental setup

The hydrodynamic cavitation setup was the same as the one used by Sarvothaman et al. [44,45], employing a small vortex-type cavitation device with a throat diameter of 6 mm. A batch assembly was used, powered with a 1 HP centrifugal pump together with two control valves to regulate the flow rate through the cavitation device (Fig. 1). Temperature was controlled with a cryostat at 16 °C. The cavitation conditions were set to the optimum ones found by Sarvothaman et al. [45] using distilled water, at a head loss of 2.8 bar. The reservoir tank was filled with 3.5 L of the corresponding solution, and the flow rate through the HC device was 5 L min^{-1}.

2.2. Effect of HC on the viscosity of a soluble polymer solution

An aqueous solution of carboxymethylcellulose (CMC) was prepared with a concentration of 0.05% w/w (Fluka p.a.) slowly dissolving the polymer in distilled water. The CMC solution was treated by HC using the setup shown in Fig. 1. Samples were taken from the initial solution and after 550 passes. Afterwards, the apparent viscosity of the CMC solution was measured at 20 °C with a plate-cone viscometer (BROOKFIELD DV-II+Pro). The apparent viscosity was determined at two shear rates, 75 and 375 Hz, using the BROOKFIELD DV-II+Pro-software. The apparent viscosity was calculated from the shear stress, which was measured in triplicate.

2.3. Effect of HC on the solubility of an ionic salt

Experiments were conducted using a subsaturated solution of $BaSO_4$ to analyze the effect of HC on the precipitation of an ionic salt. A 1 M $BaCl_2$ solution was mixed with a 1 M Na_2SO_4 solution in a proportion of 1:1.5. The precipitate formed was allowed to settle for 24 h. The clear supernatant was then filtered through 0.22 μm pore cellulose acetate filters. Then, the working solution was obtained by diluting this saturated solution in a ratio of 0.9:1 with distilled water. All the process was maintained at 16±0.2 °C using a digitally-controlled cryostat to avoid thermal effects regarding changes in the precipitation equilibrium constant. The presence of precipitated $BaSO_4$ was measured using a spectrophotometer set at 550 nm, the same used for sulfate determination by spectrophotometry from $BaSO_4$ precipitation [4].

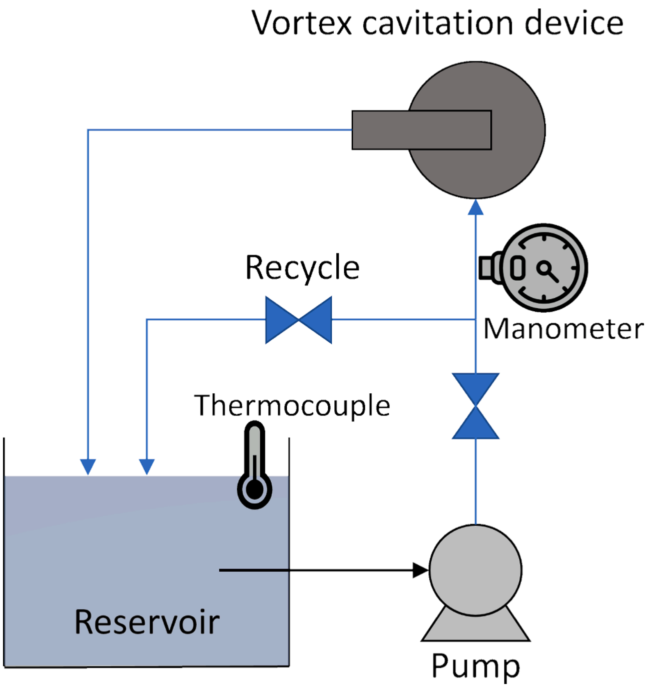

Fig. 1. Schematic of the hydrodynamic cavitation setup.

2.4. Effect of HC on the solubility of volatile organic compound (VOC)

Two solutions were employed to analyze the effect of HC on the desorption rate of VOCs dissolved in water. Diluted solutions of ethanol and hexanol (12 mM each) were used. They were subjected to HC while a continuous flow of regulated air was circulating through the reservoir tank. The concentration of alcohol in the gas outlet stream was assessed continuously. A gas retention hood coupled with a bubbler was used to generate a constant gas flow (5.00 ± 0.01 mL s^{-1}) where the alcohol concentration was continuously measured using an MQ-3 gas sensor [53]. The bubbler was placed inside the recirculation tank as shown in Fig. 2. The system was first operated keeping the HC device below the cavitation pressure or inception [45] for a certain time. Then, a 2.8 bar pressure loss was imposed through the cavitation device, leading to the optimum cavitation conditions. Afterwards, the conditions were periodically modified from non-cavitation to cavitation, while the alcohol concentration in the gas flow was continuously registered. The temperature in the reservoir, an important variable regarding gas-liquid equilibria, was monitored to ensure negligible variations.

3. Conceptual model for HC effects

3.1. Supercritical water in HC systems inferred from simulations

Numerical simulations of HC systems were carried out by Krishnan et al. [19] and Pawar et al. [39]. Simulation data of single bubble dynamics obtained by these authors were analyzed considering the phase equilibrium diagram of water (Fig. 3). SCW oxidation reactor (SCWO)

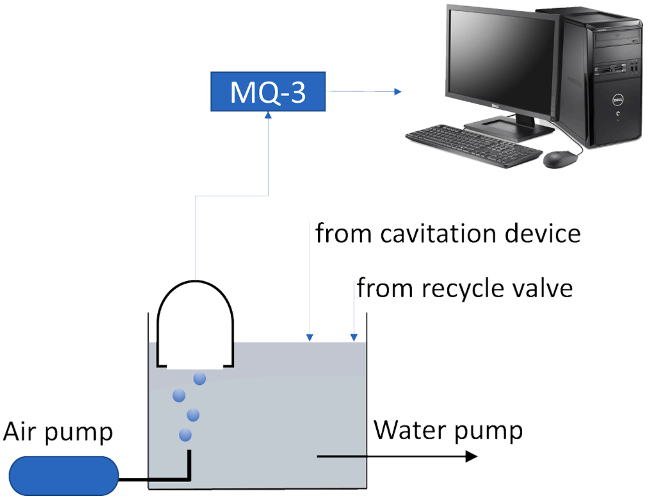

Fig. 2. Schematic of the system used for analyzing the effect of HC on VOC desorption rate.

conditions [20] have also been included in the figure for comparison.

The cavitation bubble formation and collapse go through three different stages: (1) First, when the local pressure falls below the liquid vapor pressure, a cavity is formed. This cavity, usually called “bubble”, is initially a vacuum space that is filled rather quickly with the solvent and vapor molecules of dissolved compounds, forming a bubble with very low-pressure vapor. This process is approximately represented in Fig. 3 by the green arrow. (2) Afterwards, when the formed cavities are driven farther from the cavitation device and the pressure increases, the bubble starts to collapse, imploding. During this stage, both pressure and temperature inside the bubble rise enormously. Those conditions are shown in Fig. 3 inside the implosion region. (3) Finally, once the collapse stops, the cavitation bubble disappears, leaving behind a very small gas bubble formed by the dissolved gases initially present in the solution, if applicable.

The results obtained by numerical simulations [19,39] indicate that the pressures and temperatures reached during the implosion of a cavitation bubble, whether for an orifice plate or a venturi tube, can lead to the formation of supercritical water (Fig. 3). These results are consistent with the recent findings by Pandit et al. [36], also shown in Fig. 3, who inferred SCW conditions through the application of single-bubble dynamics to a vortex-type or diode cavitation device. Hence, the reported simulations suggest that there are conditions of HC that can induce the formation of supercritical water domains.

3.2. *Conceptual model based on cavitation induced supercritical water*

A conceptual model based on the assumption of the presence of SCW domains within the cavitation bubble is sketched in Fig. 4. When considering the cavitation bubble system and the attainment of pressures and temperatures leading to supercritical water, the initially formed water-vapor interface will fade, forming a continuum from the center of the cavitation bubble to the boundary layer transition to ordinary liquid water. Furthermore, it is well known that in SCW diffusivity increases significantly. If the transformation to the supercritical state occurs on a much smaller time scale than the characteristic time scale of the cavity collapse, this rapid change will cause a substantial rearrangement of species distribution within and around the cavitation bubble prior to collapse. The main two effects will involve the expulsion of electrolytes towards the liquid phase, and the rapid transfer of hydrophobic compounds, like volatile non-polar molecules and dissolved gases, into the cavitation bubble (Fig. 4B-D). Thus, a zone of high concentration of electrolytes and polar compounds will be generated in the surrounding region of the bubble, while the interior will be enriched in hydrophobic species and dissolved gases.

Since the characteristic length of the system is extremely small (≈100 μm or less), the diffusion mechanism would be fully capable of ensuring transport during the lifetime of the cavitation bubble. Krishnan

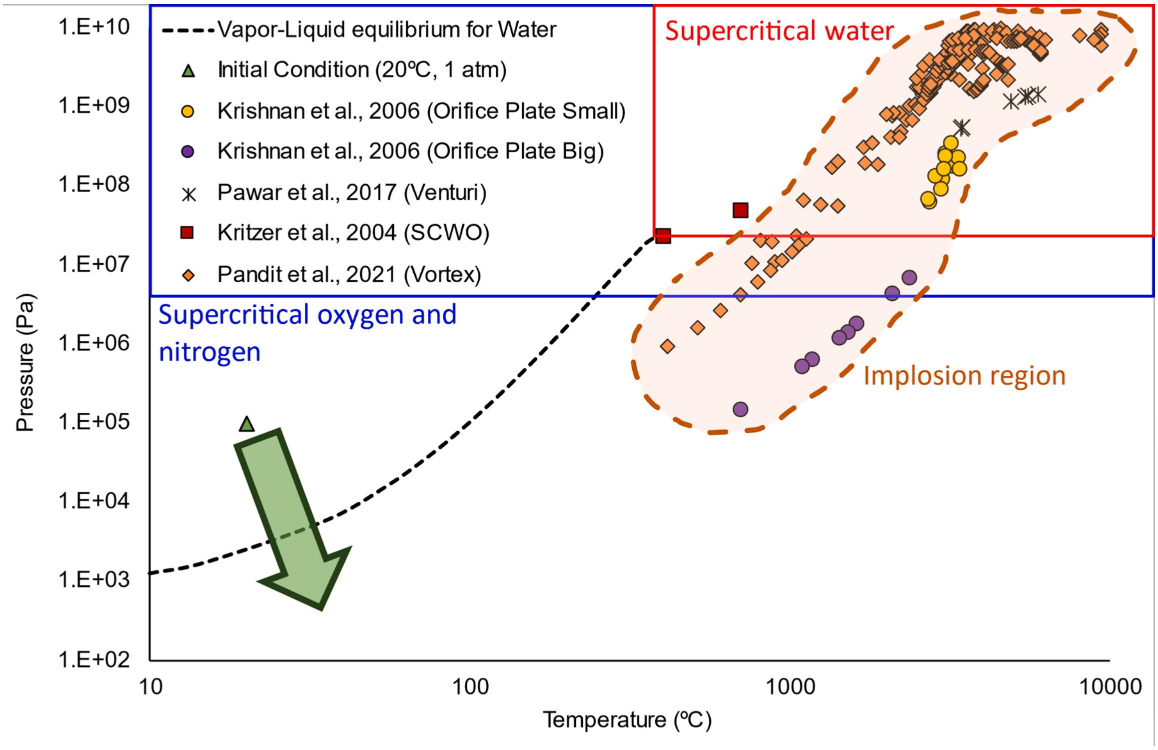

Fig. 3. Conditions reached under cavitation, as inferred from the simulation of single-bubble dynamics, represented in the water phase equilibrium diagram. Thermodynamic data for water, oxygen, and nitrogen, taken from Dean [8] and Weiss [56], are shown for comparison.

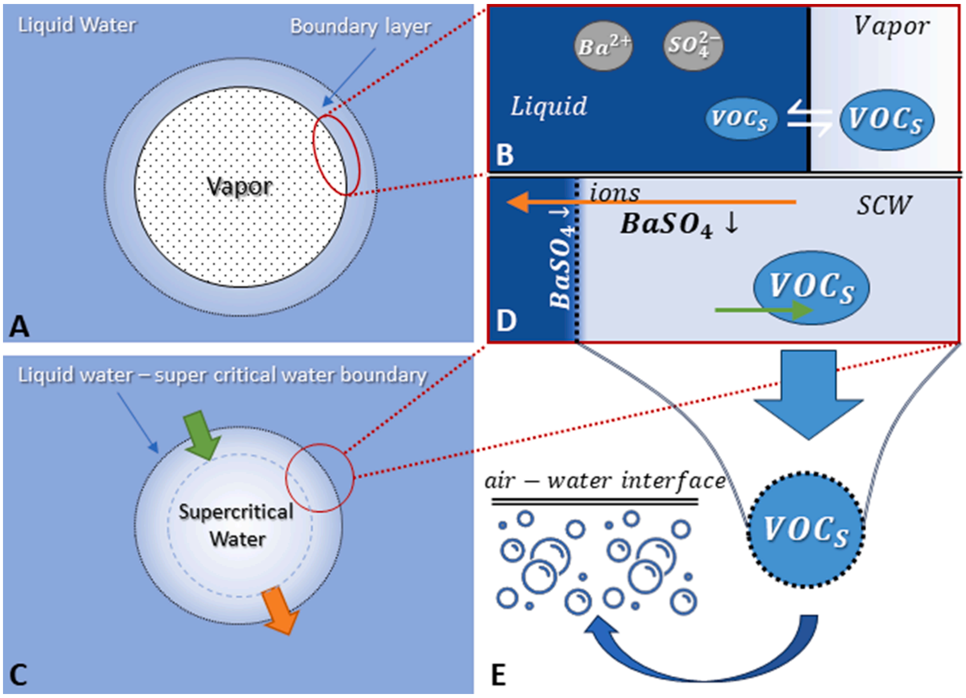

Fig. 4. Sketch of a cavity before (A – D) and after (E) collapse. A- The bubble is formed, reaching its maximum diameter; B- VOCs are driven into the bubble while ions remain in the liquid phase; C- The bubble is compressed, and temperature increases. The vapor inside the bubble and part of the surrounding liquid become supercritical, causing the original gas-liquid boundary to fade; D- Ions in the SCW phase and in the ions-enriched liquid boundary precipitate, forming a local colloidal suspension. VOCs remaining in the surrounding liquid phase diffuse into the SCW phase. E- After collapse, nanobubbles enriched with VOCs form, and may remain supersaturated in the liquid phase for a period. If they reach the gas-liquid interface, VOCs stripping is promoted. For part C and D: The green arrow indicates the displacement by diffusion of hydrophobic compounds and dissolved gases to the SCW domain, while the orange arrow indicates the transport of hydrophilic species (electrolytes) expelled into the liquid bulk.

et al. [19] found through numerical simulations that a large number of water molecules are capable of diffusing into the cavities before the collapse occurs. Then, it can be expected that, when the supercritical condition is reached, the gas-liquid equilibrium of dissolved gases has already been attained. There will be an enrichment of hydrophobic compounds, and even gas nanobubbles may be formed by dissolved gases concentrated in the SCW phase during the implosion (Fig. 4D, E). These gas nanobubbles will be in equilibrium with the SCW phase.

The formed nanobubbles saturated in gases and volatiles will be surrounded by a layer of electrolytes and polar compounds in the liquid boundary layer. In this way, concentrations in the gaseous phase would likely be higher than those corresponding to equilibrium for the ordinary liquid phase. Given the negligible turbulence within the gas phase for such small-scale lengths, it is expected that supersaturation conditions would persist for a reasonable time. The hydrophilic substances, mainly electrolytes and polar molecules, will be concentrated in the boundary layer formed around the nanobubbles; then, any chemical reaction whose rate depends on their concentration will experience a speed boost. HC would therefore induce an increase in reaction rate by locally concentrating the involved reactants.

4. Results and discussion

4.1. Effect of HC on the viscosity of a soluble polymer solution

An aqueous solution of a soluble polymer has a higher viscosity than pure water, given by the interaction between polymer molecules and water molecules, and among the polymer molecules themselves. These interactions are determined by Van der Waals forces related to functional groups present in the polymer and its average molecular weight.

Table 1 depicts the effect of HC on the viscosity of an aqueous solution of CMC (0.05%) subjected to 550 passages through the cavitation device. The viscosity significantly decreased after the HC treatment. This behavior can be explained by the reduction in the average molecular weight of the polymer that would happen when the CMC molecules break down into smaller chains. In HC systems, without the aid of hydrogen peroxide or other oxidants, the HO• concentration is very low, around 2 μMol·L^{-1} [26]. Therefore, it is hardly plausible to attribute the viscosity decrease to a radical attack that breaks down the CMC chains. Besides, the pyrolysis mechanism achieved by the high temperatures and pressures produced during bubble collapse in HC [14] would reduce the total amount of CMC rather than cutting and breaking down the CMC molecules. Moreover, to achieve pyrolysis the CMC molecules must be inside the cavitation bubble at the time of collapse, which is difficult because CMC tends to remain in the liquid phase due to its high affinity with water. Only CMC molecules located in the water-gas interface would be affected, probably to a marginal extent. Taking this into account, the existence of SCW provides a more plausible explanation. In SCW, CMC breaks down into smaller oligomers by hydrolysis [55]. At the same time, despite being less soluble in SCW than in liquid water, CMC is a large non-volatile molecule with almost negligible vapor pressure. It is considerably more probable that it transfers into a SCW domain than into the gas phase. Then, SCW would allow CMC to be inside the collapsing bubble in significantly higher quantities than in the

Table 1
Effect of HC on CMC viscosity for different shear rates.

Condition	Shear Rate (Hz)	Apparent viscosity (mPa·s)	SD (mPa·s)	% Change
Initial	75	20.87	0.63	−27.4 %
After HC		15.14	0.08	
Initial	375	5.40	0.51	−35.6 %
After HC		3.48	0.22	

gas phase. Also, the enhanced diffusion coefficients related to supercritical conditions would enhance mass transfer into the SCW-filled cavity interphase compared to the liquid-gas interface, allowing CMC to diffuse inside the cavitation bubble.

4.2. Effect of HC on the precipitation of an ionic salt

The solubility of ionic salts in SCW is considerably lower than in liquid water under atmospheric conditions. Thus, if SCW is present during the cavitation collapse, significant effects on any ion pair close to saturation will be observed. Dissolved ions remain in the liquid boundary layer when the cavitation bubble forms (Fig. 4B). When the collapse reaches supercritical water conditions, a fraction of the liquid water in the boundary layer will undergo a phase transition to SCW. In the same way, the vapor inside the bubble will become SCW. Then, the solubility of ionic salts will decrease in this region due to the significantly lower dielectric constant, and the ions present will be pushed away or precipitate (Fig. 4D). If the ions concentration were close to saturation, a precipitate of the insoluble ionic salt will form, even if the liquid bulk remains sub-saturated.

The effect of HC on a sub-saturated solution of $BaSO_4$ was studied. Results shown in Fig. 5 provide evidence of the appearance of a colloidal $BaSO_4$ precipitate, as determined from the absorbance measured at 550 nm. The absorbance increases as more precipitate is formed during the process. Once the HC started, an increase in the absorbance induced by the formation of a precipitate was immediately observed. Then, when the HC was stopped, the formed colloidal precipitate re-dissolved in the sub-saturated liquid water. After enough time, the absorbance decreased towards zero, indicating complete re-dissolution.

According to the model proposed, the extreme conditions imposed by the bubbles' collapse will lead to the appearance of SCW within the cavitation bubble and in a fraction of the surrounding liquid boundary layer. When HC is imposed and the cavitation bubble forms, the Ba^{2+} and SO_4^{2-} ions will be in the surrounding liquid boundary layer as well as in the liquid bulk. The low affinity of SCW with ions will push them towards the liquid water, away from the collapsing cavity. A boundary layer turning supercritical and concentrated in Ba^{2+} and SO_4^{2-} will be generated surrounding the collapsing bubble. Hence, precipitation of $BaSO_4$ will occur even if the liquid bulk is not saturated. The precipitate will not be at equilibrium with the liquid bulk and, in line with our findings, when HC is turned off it will re-dissolve entirely. Precipitation of an ionic salt from an unsaturated solution cannot be explained either by radical attack or by pyrolysis, which are the generally accepted mechanisms to interpret trends in HC. Hence, the existence of SCW domains provides a more plausible explanation.

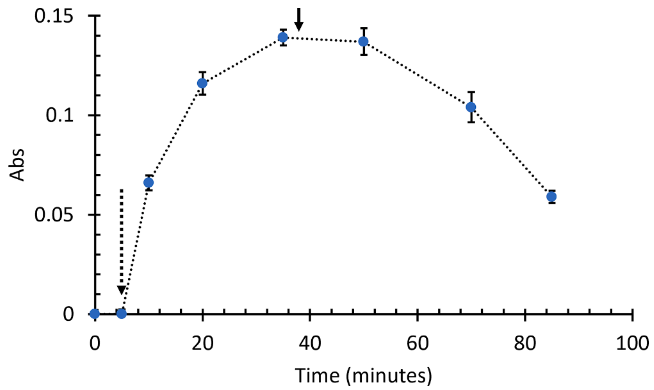

Fig. 5. Effect of HC on a sub-saturated solution of $BaSO_4$. Variation of the absorbance at 550 nm indicates the presence of a colloidal precipitate. The dotted arrow marks the start of cavitation, while the solid arrow marks the time when cavitation was turned off.

4.3. Effect of HC on the stripping of volatile organic compounds (VOCs)

Considering the results obtained for the $BaSO_4$ precipitation, pointing to the inception of supercritical conditions and the effect of SCW on ionic salts, additional experiments were performed to analyze the influence of HC on the desorption rate of VOCs. Ethanol and hexanol solutions were treated by HC as model compounds with similar functional groups and different volatilities and polar features. The concentration of alcohol in the gas stream was continuously determined with an MQ3 gas sensor, sensible to alcohols. Hence, with this system, the alcohol concentration in the gas phase was monitored while cavitation was imposed and removed, to confirm that the effect was due to HC. Results are shown in Fig. 6. Inception of HC led to an immediate increase in the amount of alcohol in the gas outlet stream, detected by the gas sensor signal rise. When HC stopped, the signal, and therefore the alcohol concentration, returned to the original value, indicating negligible variation of the alcohol concentration in the liquid phase during the experiment.

The discerned trend may be ascribed to an augmented mass transfer of alcohol, stemming from increased interfacial area and/or a heightened mass transfer coefficient. However, it could also be related to the higher alcohol solubility in SCW. As depicted in Fig. 4, when the cavity forms it is expected that the alcohol molecules will concentrate within the cavitation bubble and in the surrounding liquid boundary layer. Since the initial pressure inside the cavitation bubble is nearly zero, any volatile compound present, including the solvent (water in this case) will rapidly diffuse into it (Fig. 4B). Numerical simulations have shown that a significant amount of water molecules can diffuse before collapse starts [19]. The existence of supercritical water conditions will facilitate VOCs diffusion into the cavitation bubble (Fig. 4D). In addition, less polar compounds will have higher solubility in the SCW bubble than in liquid water, also increasing their mass transfer into the bubble. When the collapse process finishes, nanobubbles supersaturated in the VOCs could be formed (Fig. 4E). These nanobubbles will take longer to re-dissolve in water because of mass transfer limitations, particularly if they are rich in compounds that are sparingly soluble in liquid water. Moreover, if they reach the superficial water-air interface (see the bubbling system, schematized in Fig. 2), the VOC will be transferred from the liquid to the gas phase at a much higher rate than expected.

Ethanol and hexanol are VOCs and their concentration in the outlet gas stream increased significantly when cavitation was imposed. The effect was stronger on hexanol than on ethanol, as shown in Fig. 6. Although an increase in the gas-liquid interfacial area induced by HC could explain an enhanced stripping rate, the interfacial area increase should not depend on the compound. The apparent higher effect over hexanol stripping can be attributed to the lower polarity of hexanol related to the SCW conditions. Specifically, a less polar molecule like hexanol would have a higher affinity to get into the SCW bubble than ethanol and a higher limitation for re-dissolving in the liquid water before reaching the gas-liquid interface. Then, the conceptual model based on assuming a strong influence on the appearance of SCW would suggest that the lower the VOC affinity with water, the higher the effect of HC.

An interesting comparison can be made with the results reported by Taşdemir et al. [50], who have investigated hydrodynamic cavitation-aided ammonia stripping. These authors observed an enhanced removal of ammonia and attributed it to an increase in the air-water interfacial area. It is important to mention that with HC they found an improvement that was larger than that obtained under air bubbling. The decrease in ammonia concentration in the liquid phase was independent of the initial ammonia concentration, indicating a relatively high liquid mass transfer coefficient (gas control) and, therefore, negligible gradient concentration differences in the liquid phase, consistent with high solubility of ammonia in water. An increase in liquid turbulence would affect the liquid side mass transfer coefficient, which is not the rate controlling step; thus, not explaining the enhanced

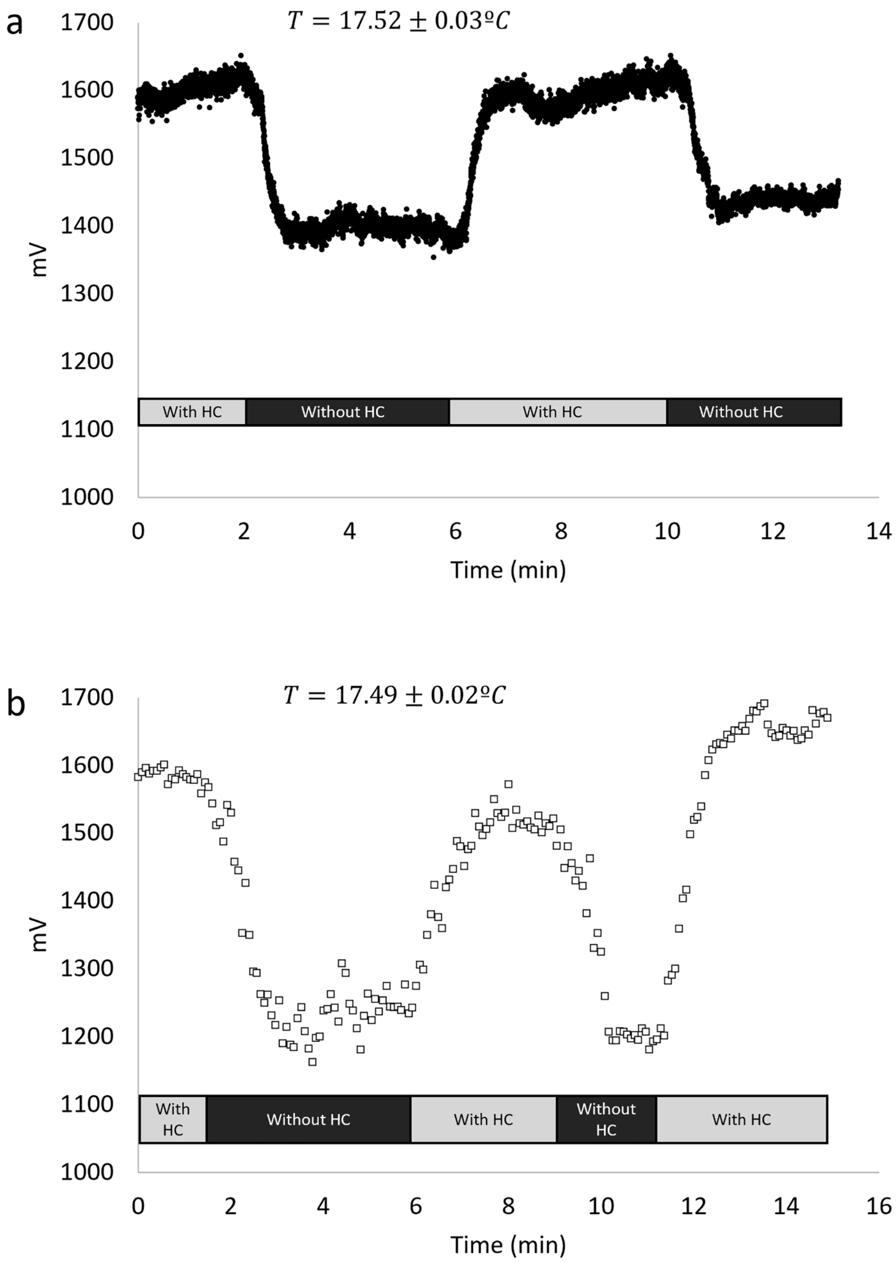

Fig. 6. Ethanol (a) and Hexanol (b) concentration in the gas phase as a function of time with and without HC. The average temperature (T) and the standard deviation are also shown for each plot.

stripping. The authors also found that the enhancement of mass transfer was inversely proportional to the cavitation number, evidencing its dependence on the cavitation collapse energy, as expected for SCW formation. According to the proposed model, nanobubbles enriched with ammonia would be produced (Fig. 4E), leading to a higher mass transfer rate. If the supersaturated gas nanobubbles reach the liquid-gas interface, the degree of stripping would be greater than the one expected considering the concentration gradient given by the liquid bulk–gas equilibrium.

According to the surface renewal theory of mass transfer [6], the mass transfer coefficient depends upon the turbulence of fluid elements or the surface renewal rate for both gas and liquid phases. In this case, however, the main transference elements would be the nanobubbles that reach the interface and convey the concentrated supersaturated compounds to the gas phase.

4.4. *Analysis of HC effects on other processes based on the postulated model*

4.4.1. *Application of HC as an AOP and catalytic-like effects of HC*

The application of HC in the oxidation of organic compounds has been widely investigated both as a standalone technique or with intensification means ([34]; Federov et al., 2022; [18,29,50,51]). Among the operational variables involved, pH has been identified as a critical aspect to consider (Federov et al., 2022; [3]). The occurrence of SCW supports the influence of pH on HC. Higher conversions are observed at low pH values, which are frequently attributed to higher radical hydroxyl generation. Changes in pH have a strong influence on the polarity of compounds and thus induce variations in the relative distribution of any compound between liquid, gas, and SCW phases. According to the model proposed, mainly the non-polar compounds will diffuse into the cavitation bubble, and they will be the most affected when a SCW domain is formed. Therefore, the conversion achieved at any given pH will depend on the speciation molar fraction of the compound.

Application of HC would not necessarily lead to an enhancement of the desired process. The optimal cavitation number must be determined from experiments. For certain conditions, the appearance of a strong positive effect of hydrodynamic cavitation could be related to the attainment of SCW. For those cases, changes in polarity due to pH will notably influence the effect of HC on the transformation of compounds with acid-base behavior. Patil et al. [38] have reported that the degradation of organic solvents by HC correlates with a decrease in the dielectric constant of the solvents. The pyrolysis of uncharged, hydrophobic, and/or non-polar substances will be favored due to their enhanced diffusion to the SCW phase.

Patil and Bhandari [37] studied the suitability of adding a solvent (1-octanol, cyclohexanol, 1-octane, or toluene) as an additive (1–5 % v/V) to intensify the removal of 4-aminophenol by conventional HC. These authors found that the addition of octanol or cyclohexanol promotes the removal of ammoniacal nitrogen while the addition of toluene or octane has the opposite effect. This suggests a competitive mechanism in which the less polar solvent molecules easily diffuse into the SCW and hinders the entrance of 4-aminophenol into the cavitation bubbles. In contrast, the alcohols, which have larger solubility in water and are more polar and less volatile than 4-aminophenol, do not interfere so strongly. Consequently, the elimination of 4-aminophenol is promoted rather than hindered. As explained in Section 4.3, the less polar a compound is, the higher is its solubility in SCW, which favors its mass transfer into the bubble and further stripping or pyrolysis.

Another often overlooked factor is the ionic strength of the solution and the type of solutes present. For an organic non-polar non-volatile compound, high ionic strength can induce a salting-out effect, increasing the compound solubility in SCW. This observation aligns with results reported by Gogate and Bhosale [13], who found an increase in dye degradation when the ionic strength was higher. Also, according to Merouani et al. [32], the addition of salts facilitates the degradation of compounds due to intensifying the collapse by reducing water vapor pressure. This effect, observed in both HC and ultrasonic cavitation, could arise from the existence of SCW domains.

Gagol et al. [12] found that the addition of H_2SO_4 led to an increase in the degradation of various organic compounds, unlike HCl and HNO_3. While some differences can be attributed to chemical reactions such as specific radicals' formation and scavenging reactions, the effect observed may also be related to the presence of SCW. At the same pH for the three acid solutions, no significant speciation effects are present, but a substantial difference in ionic strength exists. The addition of sulfuric acid may cause an increased effect of HC due to the higher ionic force that promotes the diffusion of organics into the SCW domain. Moreover, the synergistic effect of ionic radius and charge affects the solubility of salts in SCW [27], thereby contributing to the salting-out effect. It has been reported that in ultrasonic oxidation processes, high ionic strength promotes the oxidation of organic substances by directing them to the boundary layer, identified as the primary site of oxidation [32,46]. The presence of SCW enables a higher mass transfer rate and a greater concentration of organic compounds at the boundary layer, thereby enhancing oxidation and decomposition.

In the last decade, there has been a research focus on process intensification through the combination of HC and AOPs in hybrid processes, as well as the coupling of an HC device to an AOP reactor in series [3,5,10,21,30,38,41,43]. The improvements found when using HC have been attributed mainly to the enhancement of the radical generation rate and mass transfer improvements. The catalytic effect of HC to promote radical formation when adding H_2O_2 to several AOPs can also be related to the increase in diffusivity and the decrease in the dielectric constant characteristics of the inception of SCW domains. The low affinity between ions and SCW along with the faster mass transport will create a zone of high concentration of OH• in the SCW-liquid boundary, characterized by significant turbulence induced by the low viscosity. Therefore, any limitation to mass transfer and reaction between OH• and organic substances would be reduced. Also, the enhanced hydrogen peroxide decomposition in SCW [17] will favor H_2O_2 efficiency and allow an increased number of free radicals trapped in the bubble boundary layer, creating short-lived high-concentration zones where compounds can be oxidized. In addition, as H_2O_2 can decompose into oxygen at high temperatures, the SCW formed inside the cavitation bubble will be saturated in oxygen. This fact could promote pyrolytic oxidation reactions at a very high rate and efficiency, while excess oxygen may react with water to form additional free radicals in SCW [17]. Therefore, the assumption of SCW domains does not contradict, but complements the already accepted mechanisms of radicaĺs attack and pyrolysis. When SCW formation is achieved, the HC performance is improved.

4.4.2. *Intensification of other processes using HC*

Another intensification case in which HC has shown interesting results is in the extraction of valuable compounds from different raw materials [2,15,57]. Solid-liquid extraction of non-polar compounds in water is one field of great interest, such as algae lipids extraction [25, 33], and extraction of antioxidant compounds from vegetal tissues [1]. While most research effort has been directed towards efficiency analysis and comparison with other techniques, very little is known about the main mechanisms involved in HC-aided extraction. Albanese et al. [1] reported the successful water (solventless) extraction of bioactive organic molecules from pine leaves. Excellent efficiency for polyphenols and flavonoids extraction was obtained despite their low solubility in water, which had typically imposed the use of alcohols or other additives to improve the extraction [35,48]. The formation of SCW can explain these results due to the higher solubility of polyphenols and flavonoids in SCW. This effect should be considered coupled with physical effects over the solid matrix given by shear stresses and turbulence in the cavitation device. Extraction of labile compounds sparingly soluble in water cannot be explained by radical attack or pyrolysis. The SCW hypothesis provides a plausible explanation for the enhanced extraction rates found under solventless conditions.

Lee and Han [23] studied the extraction of lipids from algae with HC in a mixture of water:hexane 1:0.8. Cell disruption by shear stress and enhanced mixing was given as the main reason behind HC extraction enhancement. The presence of SCW during bubble collapse could offer another explanation for increased extraction yields, being compatible with shear-stress related enhancements. After cell rupture, the SCW would allow non-polar substances to diffuse into the cavity. If a non-polar solvent is also present, both substances would reach high concentrations in the cavitation bubble, and after the collapse would remain as liquid nano droplets. Since hexane is almost insoluble in water, a colloidal-like particulate composed of liquid hexane rich in dissolved lipids would form. When the water fraction is separated by decantation, this colloidal fraction would dissolve into the hexane bulk. This is consistent with the linear relationship found between cavitation time and lipid yield. Also, the authors found an optimum cavitation number, which could be the result of optimum SCW formation conditions.

Later, Lee and Han [24] used a Fenton-like process combined with hydrodynamic cavitation to promote the extraction of lipids from wet microalgae. No organic solvent was used during the process; hexane was used afterwards to recover the lipids from the aqueous suspension formed. They found that working at pH=3 and with 1 % hydrogen peroxide led to circa 80 % yield of the total amount of lipids in the microalgae. The presence of a SCW domain could have contributed to intensifying the lipid extraction from the algae debris, creating a lipid-water emulsion from which the lipids were readily recovered.

In line with the previous discussion, another example worth considering is the intensification of biodiesel production achievable by cavitation. It has been reported that up to 98 % reduction in reaction times can be found for the conversion of food waste into biodiesel due to the increase in mass transfer [2]. Mass transfer is a serious limitation of the process because of the liquid-liquid heterogeneous system characteristic of the alcohol-oil immiscible reagents. The presence of a SCW domain can explain the enhanced mass transfer and reactant contact achieved through cavitation to boost the biodiesel yield. Supercritical methods have proved to be quite efficient in accelerating biodiesel production from different sources [28,52].

5. Conclusion

This work proposes that the plausible thermodynamic effect of the inception of supercritical water state should be incorporated into the mechanisms commonly assumed to interpret hydrodynamic cavitation data. The suggested conceptual model can serve as a valuable tool for interpreting results, particularly in relation to enhanced mass transfer phenomena. The removal of volatile compounds, whether generated during the breakdown of larger molecules or initially present in the sample, might occur through stripping instead of oxidation. Understanding experimental trends, designing new systems, and developing future hydrodynamic cavitation models and simulations can greatly benefit from acknowledging the presence of a supercritical water phase.

Fundings

Agencia Nacional de Promoción de Ciencia y Técnica (ANPCyT), Argentina PICT2019 00955, PICT-2021-CAT-I-00086, Universidad de Buenos Aires, Argentina UBACyT 20020220100154BA.

CRediT authorship contribution statement

S.N. Fleite: Writing – original draft, Methodology, Investigation, Formal analysis, Data curation, Conceptualization. **M.A. Ayude:** Writing – review & editing, Funding acquisition, Formal analysis, Conceptualization. **V.V. Ranade:** Validation, Formal analysis, Conceptualization. **M.C. Cassanello:** Writing – review & editing, Supervision, Methodology, Funding acquisition, Conceptualization.

Declaration of competing interest

The authors declare that they have no known competing financial interests or personal relationships that could have appeared to influence the work reported in this paper.

Data availability

Data will be made available on request.

Acknowledgements

Financial support from Universidad de Buenos Aires, Argentina (UBACyT 2023 20020220100154BA) and from the National Agency for Promoting Science and Technology (ANPCyT), Argentina (PICT 2019–0955 and PICT-2021-CAT-I-00086) is gratefully acknowledged.

References

[1] L. Albanese, A. Bonetti, L.P. D'Acqui, F. Meneguzzo, F Zabini, Affordable production of antioxidant aqueous solutions by hydrodynamic cavitation processing of silver fir (Abies alba Mill.) needles, Foods 8 (2) (2019) 65.
[2] Z. Askarniya, X. Sun, Z. Wang, G. Boczkaj, Cavitation-based technologies for pretreatment and processing of food wastes: major applications and mechanisms–A review, Chem. Eng. J. 454 (2023) 140388.
[3] K.O. Badmus, N. Irakoze, O.R. Adeniyi, L. Petrik, Synergistic advance Fenton oxidation and hydrodynamic cavitation treatment of persistent organic dyes in textile wastewater, J. Environ. Chem. Eng. 8 (2) (2020) 103521.
[4] R. Baird, E. Rice, A. Eaton, Standard Methods for the Examination of Water and Wastewaters. Water Environment Federation, Chair Eugene W. Rice, American Public Health Association Andrew D. Eaton, American Water Works Association, 2017.
[5] J. Carpenter, M. Badve, S. Rajoriya, S. George, V.K. Saharan, A.B. Pandit, Hydrodynamic cavitation: an emerging technology for the intensification of various chemical and physical processes in a chemical process industry, Rev. Chem. Eng. 33 (5) (2017) 433–468.
[6] P.V. Danckwerts, Significance of liquid-film coefficients in gas absorption, Ind. Eng. Chem. 43 (6) (1951) 1460–1467.
[7] S. Das, A.P. Bhat, P.R. Gogate, Degradation of dyes using hydrodynamic cavitation: process overview and cost estimation, J. Water Process Eng. 42 (2021) 102126.
[8] J.A. Dean, Lange's Handbook of Chemistry, 15th ed, McGraw-Hill Company, New York, 1999.
[9] Y. Deng, R. Zhao, Advanced oxidation processes (AOPs) in wastewater treatment, Curr. Pollut. Rep. 1 (3) (2015) 167–176.
[10] K. Fedorov, K. Dinesh, X. Sun, R.D.C. Soltani, Z. Wang, S. Sonawane, G. Boczkaj, Synergistic effects of hybrid advanced oxidation processes (AOPs) based on hydrodynamic cavitation phenomenon–a review, Chem. Eng. J. (2022) 134191.
[11] J. Feng, S.N.V.K. Aki, J.E. Chateauneuf, J.F. Brennecke, Hydroxyl radical reactivity with nitrobenzene in subcritical and supercritical water, J. Am. Chem. Soc. 124 (22) (2002) 6304–6311.
[12] M. Gagol, E. Cako, K. Fedorov, R.D.C. Soltani, A. Przyjazny, G. Boczkaj, Hydrodynamic cavitation based advanced oxidation processes: studies on specific effects of inorganic acids on the degradation effectiveness of organic pollutants, J. Mol. Liq. 307 (2020) 113002.
[13] P.R. Gogate, G.S. Bhosale, Comparison of effectiveness of acoustic and hydrodynamic cavitation in combined treatment schemes for degradation of dye wastewaters, Chem. Eng. Process. 71 (2013) 59–69.
[14] P.R. Gogate, A.B. Pandit, A review of imperative technologies for wastewater treatment I: oxidation technologies at ambient conditions, Adv. Environ. Res. 8 (3–4) (2004) 501–551.
[15] G. Grillo, L. Boffa, A. Binello, S. Mantegna, G. Cravotto, F. Chemat, T. Dizhbite, L. Lauberte, G. Telysheva, Cocoa bean shell waste valorisation; extraction from lab to pilot-scale cavitational reactors, Food Res. Int. 115 (2019) 200–208.
[16] C.R. Holkar, A.J. Jadhav, D.V. Pinjari, A.B. Pandit, Cavitationally driven transformations: a technique of process intensification, Ind. Eng. Chem. Res. 58 (15) (2019) 5797–5819.
[17] Z. Jiang, Y. Li, S. Wang, C. Cui, C. Yang, J. Li, Review on mechanisms and kinetics for supercritical water oxidation processes, Appl. Sci. 10 (14) (2020) 4937.
[18] M. Khajeh, M.M. Amin, A. Fatehizadeh, T.M. Aminabhavi, Synergetic degradation of atenolol by hydrodynamic cavitation coupled with sodium persulfate as zero-waste discharge process: effect of coexisting anions, Chem. Eng. J. 416 (2021) 129163.
[19] J.S. Krishnan, P. Dwivedi, V.S. Moholkar, Numerical investigation into the chemistry induced by hydrodynamic cavitation, Ind. Eng. Chem. Res. 45 (4) (2006) 1493–1504.
[20] P. Kritzer, Corrosion in high-temperature and supercritical water and aqueous solutions: a review, J. Supercrit. Fluids 29 (1–2) (2004) 1–29.
[21] N.J. Lakshmi, C. Agarkoti, P.R. Gogate, A.B. Pandit, Acoustic and hydrodynamic cavitation-based combined treatment techniques for the treatment of industrial real effluent containing mainly pharmaceutical compounds, J. Environ. Chem. Eng. 10 (2022) 108349.
[22] G.L. Lee, M.C. Law, Numerical modelling of single-bubble acoustic cavitation in water at saturation temperature, Chem. Eng. J. 430 (133051) (2022) 1–19.
[23] I. Lee, J.I. Han, Simultaneous treatment (cell disruption and lipid extraction) of wet microalgae using hydrodynamic cavitation for enhancing the lipid yield, Bioresour. Technol. 186 (2015) 246–251.
[24] I. Lee, J.I. Han, Development of a pretreatment method based on Fenton-like reaction combined with hydrodynamic cavitation for lipid extraction from wet microalgae, Renew. Energy 175 (2021) 415–421.
[25] I. Lee, Y.K. Oh, J.I. Han, Design optimization of hydrodynamic cavitation for effectual lipid extraction from wet microalgae, J. Environ. (2019).
[26] P. Li, Y. Song, S. Yu, Removal of Microcystis aeruginosa using hydrodynamic cavitation: performance and mechanisms, Water Res. 62 (2014) 241–248.
[27] X. Li, X. Qi, L. Lu, J. Zhao, H. Jin, Z. Ge, Y. Chen, L. Guo, Experimental and molecular dynamics simulation study on solubility characteristics of chloride and sulfate salts in supercritical water, J. Supercrit. Fluids 205 (2024) 106150.
[28] P. Maheshwari, M.B. Haider, M. Yusuf, J.J. Klemeš, A. Bokhari, M. Beg, A. Al-Othman, R. Kumar, A.K. Jaiswal, A review on latest trends in cleaner biodiesel production: role of feedstock, production methods, and catalysts, J. Clean. Prod. 355 (2022) 131588.
[29] G. Mancuso, M. Langone, G. Andreottola, A critical review of the current technologies in wastewater treatment plants by using hydrodynamic cavitation process: principles and applications, J. Environ. Health Sci. Eng. 18 (2020) 311–333.
[30] R. Merdoud, F. Aoudjit, L. Mouni, V.V. Ranade, Degradation of methyl orange using hydrodynamic Cavitation, H_2O_2, and photo-catalysis with TiO_2-Coated glass Fibers: key operating parameters and synergistic effects, Ultrason Sonochem. (2024) 106772.
[31] S. Merouani, O. Hamdaoui, Y. Rezgui, M. Guemini, Theoretical estimation of the temperature and pressure within collapsing acoustical bubbles, Ultrason Sonochem. 21 (1) (2014) 53–59.
[32] S. Merouani, O. Hamdaoui, F. Saoudi, M. Chiha, Sonochemical degradation of Rhodamine B in aqueous phase: effects of additives, Chem. Eng. J. 158 (3) (2010) 550–557.

[33] R. Mittal, V.V. Ranade, Intensifying extraction of biomolecules from macroalgae using vortex based hydrodynamic cavitation device, Ultrason. Sonochem. 94 (2023) 106347.

[34] A.V. Mohod, A.C.S.C. Teixeira, M.V. Bagal, P.R. Gogate, R. Giudici, Degradation of organic pollutants from wastewater using hydrodynamic cavitation: a review, J. Environ. Chem. Eng. (2023) 109773.

[35] P.R. More, A.R. Jambrak, S.S. Arya, Green, environment-friendly and sustainable techniques for extraction of food bioactive compounds and waste valorization, Trends Food Sci. Technol (2022).

[36] A.V. Pandit, V.P. Sarvothaman, V.V. Ranade, Estimation of chemical and physical effects of cavitation by analysis of cavitating single bubble dynamics, Ultrason. Sonochem. 77 (2021) 105677.

[37] P.B. Patil, V.M. Bhandari, Solvent-assisted cavitation for enhanced removal of organic pollutants-Degradation of 4-aminophenol, J. Environ. Manage. 311 (2022) 114857.

[38] P.B. Patil, V.M. Bhandari, V.V. Ranade, Improving efficiency for removal of ammoniacal nitrogen from wastewaters using hydrodynamic cavitation, Ultrason. Sonochem. 70 (2021) 105306.

[39] S.K. Pawar, A.V. Mahulkar, A.B. Pandit, K. Roy, V.S. Moholkar, Sonochemical effect induced by hydrodynamic cavitation: comparison of venturi/orifice flow geometries, AIChE J. 63 (10) (2017) 4705–4716.

[40] V.V. Ranade, V.M. Bhandari, S. Nagarajan, V.P. Sarvothaman, A.T. Simpson, Hydrodynamic Cavitation: Devices, Design and Applications, John Wiley & Sons, 2022.

[41] K. Roy, V.S. Moholkar, p–nitrophenol degradation by hybrid advanced oxidation process of heterogeneous Fenton assisted hydrodynamic cavitation: discernment of synergistic interactions and chemical mechanism, Chemosphere 283 (2021) 131114.

[42] V.K. Saharan, M.A. Rizwani, A.A. Malani, A.B. Pandit, Effect of geometry of hydrodynamically cavitating device on degradation of Orange-G, Ultrason. Sonochem. 20 (2013) 345–353.

[43] G. Salierno, S. Napoleone, M.A. Maisterrena, M. Cassanello, M. Pellasio, L. Doumic, M.A. Ayude, Continuous heterogeneous fenton-type process for dye pollution abatement intensified by hydrodynamic cavitation, Ind. Eng. Chem. Res. 60 (2021) 16653–16664.

[44] V.P. Sarvothaman, S. Nagarajan, V.V. Ranade, Treatment of solvent-contaminated water using vortex-based cavitation: influence of operating pressure drop, temperature, aeration, and reactor scale, Ind. Eng. Chem. Res. 57 (2018) 9292–9304.

[45] V.P. Sarvothaman, A.T. Simpson, V.V. Ranade, Modelling of vortex based hydrodynamic cavitation reactors, Chem. Eng. J. 377 (2019) 119639.

[46] J.D. Seymour, R.B. Gupta, Oxidation of aqueous pollutants using ultrasound: salt-induced enhancement, Ind. Eng. Chem. Res. 36 (1997) 3453–3457.

[47] B.K. Sreedhar, S.K. Albert, A.B. Pandit, Computation of erosion potential of cavitation bubble in an ultrasonic pressure field, J. Pure Appl. Ultrason. 39 (2017) 60–69.

[48] X. Sun, W. You, Y. Wu, Y. Tao, J.Y. Yoon, X. Zhang, X. Xuan, Hydrodynamic cavitation: a novel non-thermal liquid food processing technology, Front. Nutr. 9 (2022) 843808.

[49] K.S. Suslick, N.C. Eddingsaas, D.J. Flannigan, S.D. Hopkins, H. Xu, The chemical history of a bubble, Acc. Chem. Res. 51 (2018) 2169–2178.

[50] A. Taşdemir, İ. Cengiz, E. Yildiz, Y.K. Bayhan, Investigation of ammonia stripping with a hydrodynamic cavitation reactor, Ultrason. Sonochem. 60 (2020) 104741.

[51] P. Thanekar, P. Gogate, Application of hydrodynamic cavitation reactors for treatment of wastewater containing organic pollutants: intensification using hybrid approaches, Fluids 3 (2018) 98.

[52] L.J. Vernier, A.L.B. Nunes, M. Albarello, F. de Castilhos, Continuous production of fatty acid methyl esters from soybean oil deodorized distillate and methyl acetate at supercritical conditions, J. Supercrit. Fluids 186 (2022) 105603.

[53] H.G.J. Voss, J.J.A. Mendes Júnior, M.E. Farinelli, S.L. Stevan Jr, A prototype to detect the alcohol content of beers based on an electronic nose, Sensors 19 (2019) 2646.

[54] M. Wang, W. Yuan, Modeling bubble dynamics and radical kinetics in ultrasound induced microalgal cell disruption, Ultrason. Sonochem. 28 (2016) 7–14.

[55] N. Wei, D. Xu, B. Hao, S. Guo, Y. Guo, S. Wang, Chemical reactions of organic compounds in supercritical water gasification and oxidation, Water Res. 190 (2021) 116634.

[56] A. Weiss, Algorithms for the calculation of moist air properties on a hand calculator, Trans. ASAE 20 (1977) 1133–1136.

[57] Z. Wu, D.F. Ferreira, D. Crudo, V. Bosco, L. Stevanato, A. Costale, G. Cravotto, Plant and biomass extraction and valorisation under hydrodynamic cavitation, Processes 7 (2019) 965.